



تأثیرات اندازه دریچه اکسیدی بر عملکرد داخلی لیزر کاواک قائم گسیل سطحی ۹۸۰ نانومتری

زهرا دانش کفترودی

گروه علوم مهندسی، دانشکده فنی و مهندسی شرق گیلان، دانشگاه گیلان

چکیده: یک مسئله مهم در لیزر کاواک قائم گسیل سطحی با تحدید اکسیدی، جمع شدگی جریان در لبه دریچه است، که منجر به اتلافهای اضافی و برانگیختگی مدهای عرضی ناخواسته مرتبه بالاتر می شود. در این مطالعه، نتایج شبیه سازی سه بعدی خودسازگار الکتریکی، اپتیکی و حرارتی لیزر کاواک قائم گسیل سطحی ۹۸۰ نانومتری ارائه شده اند. تاثیر اندازه دریچه اکسیدی بر جمع شدگی جریان افزاره به صورت تئوری بررسی شده است. پس از آن تأثیرات جمع شدگی جریان بر فیزیک داخلی لیزر، مورد بحث قرار گرفته اند.

کلید واژه- جمع شدگی جریان، دریچه اکسیدی، گرمای ژول، لیزر کاواک قائم گسیل سطحی.

The Effects of oxide aperture size on the 980 nm vertical cavity surface emitting laser internal performance

Z. Danesh Kaftroudi

Department of Engineering sciences, Faculty of Technology and Engineering East of Guilan, Guilan University

Zahraadanesh@guilan.ac.ir

Abstract- An important problem for oxide confined vertical cavity surface emitting laser is current crowding at the edge of the aperture, which leads to extra losses and excitation of unwanted higher-order transverse modes. In this study, the results of self- consistently three dimensional electrical, optical and thermal simulations of 980 nm vertical cavity surface emitting laser are presented. Effect of oxide aperture size on current crowding of the device is investigated theoretically. Then the effects of the current crowding on the internal laser performance are discussed.

Keywords: Current crowding, Oxide aperture, Joule heating, vertical cavity surface emitting laser.

1 Introduction

The vertical cavity surface emitting laser (VCSEL) has become an efficient power light source in optical storage, gas detection, high bit rate data transmission, optical interconnection, and supercomputing, due to its advantages, such as low cost, low power consumption, small size, single longitude mode operation, and high speed modulation. The 980-nm VCSEL has usually been used for pumping the solid state and fiber laser. In recent years, great progress has been achieved in this field, and there have been extensive applications in short distance optical networks.

Many different approaches for achieving transverse optical and current confinement in VCSELs exist, each with its own specific advantages and draw backs. Oxide layers formed by the selective wet oxidation of aluminum rich $\text{Al}_x\text{Ga}_{1-x}\text{As}$ layers have many applications in semiconductor lasers.

For VCSELs with epitaxial grown doped semiconductor distributed Bragg reflectors (DBRs), such as the ones presented in this article, the top metal contact is usually designed in a circle, leaving the center of the topmost DBR layer free from metal. This contact shape leads to an inhomogeneous lateral current density distribution inside the top DBR. In VCSELs with current confining oxide apertures, e.g. oxide confined VCSELs; the oxide aperture is typically smaller than the diameter of the top metal contact ring in order to prevent the metal contact from blocking and absorbing the light. This leads to current crowding at the edge of the oxide aperture where the current density is much higher than the center of the conducting aperture, which may negatively impact on the VCSEL performance by inhomogeneous heating resulting in a thermal lens or spatial hole burning. Current crowding is an important issue in VCSELs [1].

Optoelectronic devices have received great attention in recent years; the complexity of physical mechanisms within such devices makes computer simulation an essential tool for performance analysis and design optimization. Advanced software tools have been developed for optoelectronic devices and several commercial software providers have emerged. These tools enable engineers and scientists to design and understand even more sophisticated nanostructure devices.

In this paper, the effect of oxide aperture size on internal physics of 980 nm VCSEL is theoretically investigated by using simulation software PICS3D which self-consistently combines 3D simulation of

carrier transport, self-heating and optical waveguiding.

2 Theoretical Model

A three-dimensional laser model, which combines carrier transport, optical gain computation, waveguiding and heat-flux, is employed in PICS3D (Photonic Integrated Circuit Simulator in 3D) [2].

2.1 Electrical Model

The electrical behaviour of the semiconductor device is described with finite- element drift-diffusion model in this package:

$$-\nabla \cdot \left(\frac{\epsilon_0 \epsilon_{dc}}{q} \nabla V \right) = -n + p + N_D(1 - f_D)$$

$$-N_A + \sum_j N_t (\delta_j - f_{tj}) \quad (1)$$

$$\begin{aligned} \nabla \cdot \mathbf{J}_n - \sum_j R_n^{tj} - R_{sp} - R_{st} - R_{Aug} + G_{opt}(t) \\ = \frac{\partial n}{\partial t} + N_D \frac{\partial f_D}{\partial t} \end{aligned} \quad (2)$$

$$\begin{aligned} \nabla \cdot \mathbf{J}_p + \sum_j R_p^{tj} + R_{sp} + R_{st} + R_{Aug} - G_{opt}(t) \\ = -\frac{\partial p}{\partial t} + N_A \frac{\partial f_A}{\partial t} \end{aligned} \quad (3)$$

The model is primarily governed by three equations. One is Poisson's equation, shown in Equation (1). The others are current continuity equation for electrons and hole shown in Equation (2) and (3), respectively. In equation (1) ϵ_0 and ϵ_{dc} are dielectric constants of vacuum and relative dielectric constant, respectively. Also n and p are electron and hole concentrations. N_D and N_A are doping densities of shallow donors and shallow acceptors. N_{tj} is density of j^{th} deep trap, f_D and f_A are occupancies of donor and acceptor levels and f_{tj} is occupancy of the j^{th} deep trap level. In Equations (2) and (3) G_{opt} is the photon generation rate per unit volume. Also R_{st} , R_{sp} and R_{Aug} are stimulated, spontaneous and Auger recombination emission rate, respectively.

2.2 Optical Model

The software solves the scalar Helmholtz equation

$$\frac{\partial^2 \varphi}{\partial x^2} + \frac{\partial^2 \varphi}{\partial y^2} + (k^2 - \beta^2)\varphi = 0 \quad (4)$$

Where $\varphi(x, y)$ represents any transverse component of the optical field, k is the absolute value of the wave vector and β is the longitudinal propagation constant. The lateral optical components are given by Bessel functions which are adjusted to measured VCSELs near fields.

2.3 Heat Generation and Dissipation

For the thermal simulation, software solves the steady-state heat flux equation.

$$\rho_L C_L \frac{\partial T}{\partial t} = -\nabla \cdot \mathbf{J}_{Heat} + H_{heat} \quad (5)$$

Which ρ_l is physical density; C_L is specific heat of crystal lattice and H_{heat} is heat source. The heat source can be separated into contributions from Joule heat, generation / recombination heat, absorption heat and Thomson heat.

3 VCSEL Structure

Figure 1 shows a schematic of the structure for a 980 nm VCSEL. The epitaxial VCSEL structure was grown on GaAs substrate. For this structure the bottom n-type distributed Bragg reflector (DBR) mirror consists of 26 pairs of quarter wavelength GaAs/AlAs layers. The top p-type DBR has 25 pairs of GaAs/Al_{0.75}Ga_{0.25}As layers. The cavity contains two In_{0.2}Ga_{0.8}As quantum wells (QWs) with GaAs barriers. The quantum wells stack is sandwiched between undoped Al_{0.42}Ga_{0.58}As spacer layers, which act as a waveguide. On the p-side of the structure, the oxide layer is not intentionally doped.

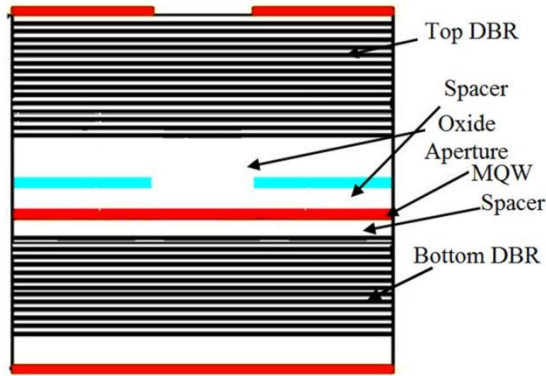


Figure 1: Schematic of a 980 nm VCSEL structure

3 Simulation Results

Figure 2 shows the optical wave intensity and the vertical current density versus radius in the top quantum well for 1.5 μm oxide aperture diameter device. As seen in Figure 2, the fundamental optical mode confines in the central region of the device, but the maximum of current density occurs near the oxide aperture edge. Thus, the gain in the quantum wells, which is always higher towards the edge of the active region mesa due to current crowding, overlaps less with the optical field of the fundamental mode. This has a negative impact on device performance. Vertical current densities in lateral position for devices with different oxide aperture diameters are compared in Figure 3. By considering this Figure, we notice that by increasing the aperture diameter, vertical current density decreases near the aperture rim, therefore the current crowding significantly decreases.

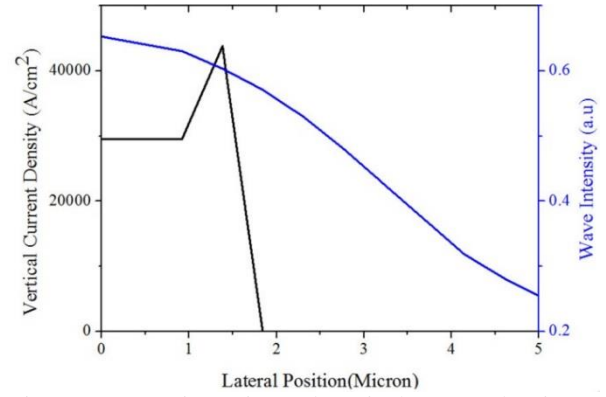


Figure 2: Wave intensity and vertical current density versus radius for 1.5 μm oxide aperture diameter VCSEL ($I=4\text{mA}$)

The current crowding in 1.5 μm VCSELs is worse than other VCSELs which explain why the 1.5 μm VCSEL has lowest output power [3]. Reduced efficiency for small apertures can be explained by a reduction of the active volume and photon number combined with stronger heating inherent to the current crowding.

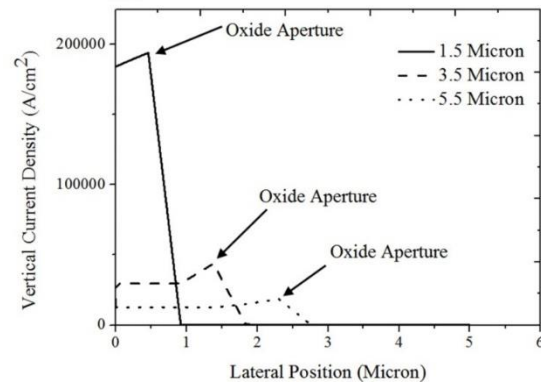


Figure 3: Vertical current density versus radius for VCSELs with different oxide aperture diameters ($I=4\text{mA}$)

Reduction of photon number by decreasing the aperture size can be seen in Figure 4.

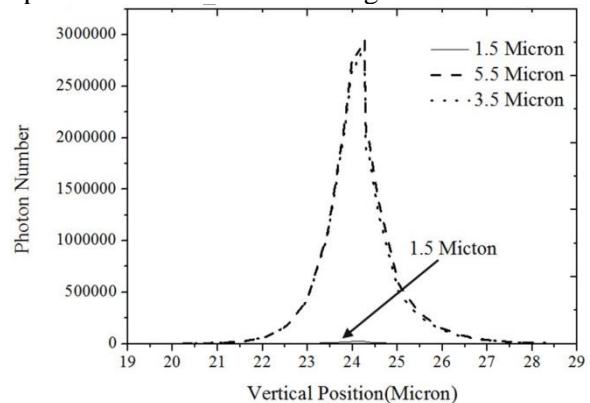


Figure 4: Photon number in vertical position for VCSELs with different oxide aperture diameters ($I=4\text{mA}$)

As current is injected into the laser diode, Joule heating occurs due to semiconductor material

intrinsic resistance and the resistance at the heterojunction interfaces. The discontinuity of band structure at heterojunction interface contributes a larger portion of the series resistance. Holes have lower mobility than electrons so that p-type material has higher electrical resistance than n-type layers. Figures 5, 6 and 7 show the 2 dimensional joule heating distribution in VCSEL with 1.5 μ m, 3.5 μ m and 5.5 μ m, respectively.

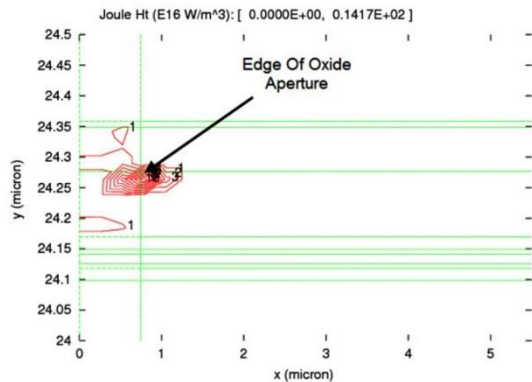


Figure 5: 2 Dimensional Joule heating distribution in VCSEL with 1.5 μ m oxide aperture ((I=4mA)

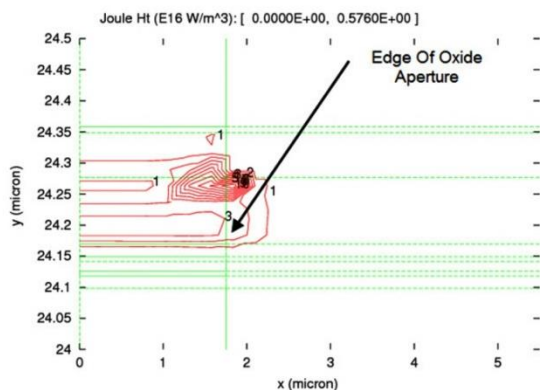


Figure 6: 2 Dimensional Joule heating distribution in VCSEL with 3.5 μ m oxide aperture ((I=4mA)

By considering these Figures, we notice that heat is blocked by the oxide and heat spreading from the upper semiconductor DBRs is limited. Smaller devices suffer more from self-heating problem because higher resistance generates more Joule heat and smaller aperture limits upward heat flow. In active region, heat is dissipated where non-radiative recombination and absorption of spontaneous emission happen. Joule heating is resistive in nature, and happens in the p-type and n-type spacer layers, cap layer and DBR. Since the active layer is comparatively thin, so Joule heating in this layer is usually neglected.

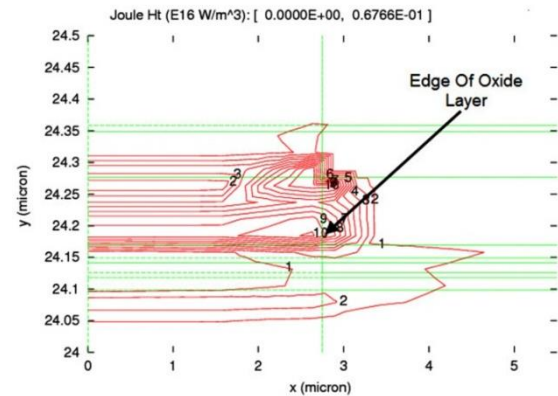


Figure 7: 2 Dimensional Joule heating distribution in VCSEL with 5.5 μ m oxide aperture ((I=4mA)
These results are in good agreement with experimental reports [4].

4 Conclusion

In this paper, the effect of oxide aperture size on internal physics of 980 nm VCSEL is theoretically investigated. Simulation results show that current crowding increases by decreasing oxide aperture size and the overall electrical resistance increases when oxide layer diameter is decreased, leading to increased resistive Joule heating.

Acknowledgements

I express my sincere appreciation to the managers of Cross Light Inc. for providing us with the advanced three-dimensional PICS3D simulation program (version 2008.12) and their kind support

References

- [1] J. Piprek, *Optoelectronic Devices: Advanced Simulation And Analysis*, Springer, 2005.
- [2] Z. Danesh Kaftroudi, E. Rajaei, and A. Mazandarani, "SIMULATION OF A SINGLE-MODE TUNNEL-JUNCTION-BASED LONG-WAVELENGTH VCSEL", *Journal of Russian Laser Research*, Volume 35, Number 2, pp. 124–137, 2014.
- [3] Z. Danesh Kaftroudi, "The effects of changes in the characteristics of the oxide aperture on 980 nm vertical cavity surface emitting performance", *23rd IPM Physics Spring Conference Institute for Research in Fundamental Sciences*, Tehran, Iran, 2016.
- [4] P. Moser, J. A. Lott, G. Larisch, and D. Bimberg, "Impact of the Oxide- Aperture Diameter on the Energy-efficiency, Bandwidth, and Temperature -Stability of 980-nm VCSELs", *IEEE Journal of Lightwave Technology*, vol. 33, no. 4, pp. 825831, 2015.